Proceedings of the 2006 IEEE/RSJ
International Conference on Intelligent Robots and Systems
October 9 - 15, 2006, Beijing, China

Forward/Inverse Models using Global Coordinates for Analytical Design of Compliant Mechanisms

Chao-Chieh Lan
Department of Mechanical engineering
National Cheng Kung University
Tainan, Taiwan 701
cclan@mail.ncku.edu.tw

Kok-Meng Lee
The George W. Woodruff School of Mechanical Engineering
Georgia Institute of Technology
Atlanta, GA 30332 –0405
kokmeng.lee@me.gatech.edu

Abstract **– The analysis of compliant mechanisms has traditionally based on known initial shapes and external forces. For applications, it is often required to find an initial shape for the specified deformed shape of the mechanism. We present here the global coordinate model (GCM) with a numerical solver that is capable of forward and inverse analysis. The model uses the arc length as the independent variable so that the shape of straight and curved links can be easily expressed. The resulting governing equations are a generalization of Timoshenko's beam theory that accounts for the effects of bending and shear deformations on large-deflected links. The effect of shear deformation on link deflection will also be investigated. Systematic procedures are developed to analyze generic compliant mechanisms. Both forward and inverse illustrations are presented. Their applications for robotic handling of bio-material are also shown. It is expected that the proposed model can give more insight on the analysis and design of compliant mechanisms.**

Index Terms – Compliant mechanisms, forward and inverse analyses, shooting method, Timoshenko's beam theory

I. INTRODUCTION

Compliant mechanisms consist of links that are sensibly deformable. The analyses of compliant links require a model that can account for the geometric nonlinearity caused by large deflection. Existing models for analyzing compliant mechanisms can be divided into lumped and distributed models. Lumped-parameter models decompose the compliant link into a rigid link and a torsional spring, such as the pseudo-rigid-body model [1]. Distributed-parameter models discretize the link into small segments and use the finite element (FE) method for analysis. Among them, the co-rotational procedure [2] has been used widely by FM software such as ANSYS. However, small time/mesh sizes are required in order to obtain very accurate results. The absolute nodal coordinate formulation [3] is frequently used for dynamic analysis. It uses global coordinates and slopes to describe the shape of the link. The resulting mass matrix is constant. However, the stiffness matrix and elastic forces are highly nonlinear.

The above methods provide an analytical tool for solving problems of compliant mechanisms; the deflected shape is analyzed given an initial shape and external loads. However, many engineering applications require both forward and inverse analyses. Unlike linear problems, where inverse solutions can be obtained by matrix inversion, large-deflection problems are nonlinear and their inverse problems are usually difficult to deal with. Stack *et al.* [4] studied the inverse elastica problem of a beam where the load and link shape are solved given the tip location. Saggere and Kota [5] studied the inverse problems of a compliant four-bar mechanism. However, these studies are limited to specific mechanisms. There is a need for a systematic formulation for solving the inverse problems of generic compliant mechanisms.

The generalized shooting method (GSM) has been developed in [6] to analyze compliant mechanisms that are governed by ordinary differential equations (ODE's). It is a generalization of shooting method [7] that deals with more than one set of independent ODE's. The shooting method treats a boundary problem as an initial value problem provided appropriate initial guesses. Its advantages over other existing methods were highlighted [8]. However, for mechanisms consist of large number of links, appropriate initial guesses may be difficult to make as wrong initial guesses will lead to unbounded solutions before completing the integration. This problem results from relatively lengthy integration interval, which leads to the idea of multiple shootings [7] that shorten the interval of integration. We develop the generalized multiple shooting method in this paper as an improved technique to deal with multiple links.

In this paper, we present the formulation of the global coordinate for modeling the kinematics and static forces of compliant mechanisms; serial and parallel configurations are considered. For design and analysis, both the forward and inverse models are needed. The forward model solves for the deformed configuration and the internal joint forces given its initial configuration and external forces. It is useful for analyzing mechanisms with known initial shapes. The inverse model, on the other hand, seeks for the initial configuration for a specified (or desired) deformed configuration. As will be shown through an example, the forward and inverse models are useful bases for analyzing compliant mechanisms with initially curved links.

The remainder of this paper provides the following:

1. We present the global coordinate model to characterize the nonlinear deflection of compliant mechanisms. This model accounts for the effects of flexural and shear deformation on the deflection. Unlike traditional models that formulate using local frames (one for each link), this model is derived using the global coordinate which requires no transformation matrices between links.
2. We develop a systematic procedure for formulating the forward and inverse models along with an improved numerical method, which is referred here as the generalized multiple shooting method (GMSM), to solve the forward and inverse problems based on GCM.

1-4244-0259-X/06/$20.00 ©2006 IEEE

Three examples are given to demonstrate the application of the GCM-GMSM to design compliant mechanisms. Specifically, the 2nd illustrates how a compliant grasper can be used to handle bio-materials, live product or natural objects. Handling of these often requires compliant devices since variability in natural products is usually several orders-of-magnitude higher than that for manufactured goods. The variability deforms compliant mechanisms to adapt to natural objects so as not to cause damage to them.

II. Global Coordinate Model (GCM)

Consider a typical mechanism consisting of ℓ compliant links shown in Fig. 1, where $\mathbf{F}_k=(F_{xk}, F_{yk})$ is an external concentrated force acting at the k^{th} joint; and s_i denotes the path length describing the shape of the i^{th} link with arrow indicating the positive direction. As will be shown, the use of s_i makes the formulation relatively easy to account for large-deflected and initially curved links.

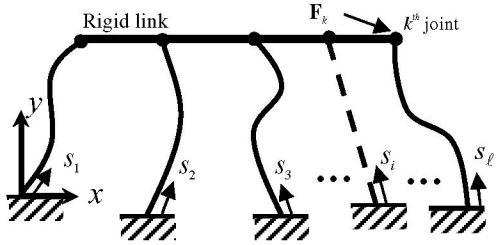

Fig. 1 A compliant mechanism

Without losing the generality, we consider here two joint configurations, which can be either clamped or revolute.

A *floating joint* connects w links as shown in Fig. 2(a). Index j is used to number the links. An external concentrated force (F_{xk}, F_{yk}) may apply at the joint.

A *fixed joint* connects a link to ground (rigid structure) as shown in Fig. 2(b). If more than one link are connected, they are treated as individual fixed joints.

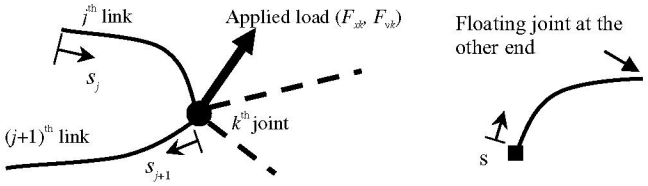

(a) Floating joint (b) Fixed joint

Fig.2 Two type of joints

II.1 Governing Equations

Figure 3 shows the i^{th} compliant link of the mechanism (Fig. 1). The link (with length L_i), which can be connected to a floating or fixed joint at both ends, deflects under external forces F_x and F_y. The original (dotted) and deflected (solid) shapes are described by the angles of rotation $\eta_i(s_i)$ and $\psi_i(s_i)+\gamma_i(s_i)$ respectively, where ψ_i is caused by flexural deformation and γ_i by shear deformation. The initial and deformed coordinates of the link are described by $(\bar{x}_i, \bar{y}_i)$ and (x_i, y_i) respectively. We first formulate the potential energy of the i^{th} link as

$$V_i = \frac{1}{2}\int_0^{L_i}[EI_i(\frac{d\psi_i}{ds_i}-\frac{d\eta_i}{ds_i})^2+\kappa_i GA_i\gamma_i^2]ds_i - F_x[x_i(L_i)-\bar{x}_i(L_i)] - F_y[y_i(L_i)-\bar{y}_i(L_i)]+F_x[x_i(0)-\bar{x}_i(0)]+F_y[y_i(0)-\bar{y}_i(0)] \quad (1)$$

where E and G are the moduli of elasticity and shear respectively; I_i is the moment of area; A_i is the cross-section area; and the shear correction factor κ_i is introduced to correct the assumption made in (1) that the shear angle γ_i is constant for the entire cross-section. The value of κ_i depends on the shape of the cross-section. The 1st and 2nd terms in the integral are the strain energy due to bending and shear respectively. The axial deformation is assumed negligible.

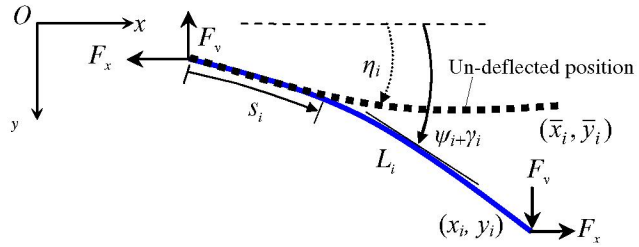

Fig. 3 The i^{th} link in a compliant mechanism

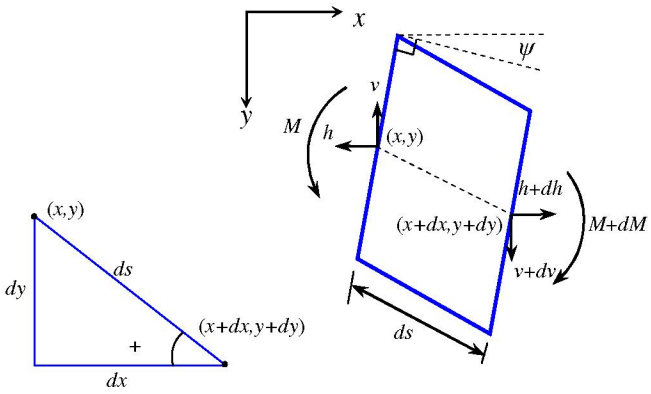

(a) Trigonometric relation (b)Infinitesimal segment

Fig. 4 Schematic of an infinitesimal segment

In Fig. 4(a), the infinitesimal path length ds is related to the differential segment dx and dy by $\cos(\psi+\gamma)$ and $\sin(\psi+\gamma)$ respectively. Using these relations, we apply the principle of minimum potential energy to (1). The equations governing the static deformation of the link can then be obtained after procedures of variational calculus as follows:

$$(EI_i/L_i^2)(\psi_i''-\eta_i'')+v_i\cos(\psi_i+\gamma_i)-h_i\sin(\psi_i+\gamma_i)=0 \quad (2a)$$

$$h_i = F_x\ ;\ v_i = F_y \quad (2b,c)$$

$$[v_i\cos(\psi_i+\gamma_i)-h_i\sin(\psi_i+\gamma_i)]-\kappa_i GA_i\gamma_i=0 \quad (2d)$$

Equation (2) is normalized to L_i by using non-dimensional path length $u_i = s/L_i$, $u_i \in [0\ 1]$ where a prime over the variable denotes 1st derivative w.r.t. u_i. The Lagrange multipliers h_i and v_i are internal forces (sum of internal stresses over cross-section) of the link in the $+x$ and $+y$ direction. Note that for clarity we assume constant E, I, G, and A in (2). The extension to non-homogenous material properties is straightforward.

Compared with many other displacement-based models that often need a post computation in order to obtain internal forces, Equation (2) can directly solve for those forces. They also serve as an essential basis for a forward/inverse model. Note that the

well-known Timoshenko's beam equations assume small deflection, i.e., $\psi \approx 0$ and $s \approx x$. Hence (2) can be viewed as a generalization of Timoshenko's equations for large-deflection analysis.

Depending on the type of problems, (2a)~(2d) must be solved simultaneously with

$$\text{Forward:} \quad \begin{aligned} x_i' - L_i \cos(\psi_i + \gamma_i) &= 0; \\ y_i' - L_i \sin(\psi_i + \gamma_i) &= 0 \end{aligned} \qquad (2e,f)$$

$$\text{Inverse:} \quad \bar{x}_i' - L_i \cos\eta_i = 0 \; ; \; \bar{y}_i' - L_i \sin\eta_i = 0 \qquad (2g,h)$$

The notation used here is similar to Frisch-Fay's model [9] for a single beam. However, the external force and its direction in F.-F.'s model are measured in the local frame attached to each link. The GCM decomposes the external force into the global x and y directions and thus requires no local frame. As only a single coordinate (inertia) frame is sufficient to model all the links, the GCM simplifies the formulation and eliminates computation of coordinate transformation.

II.2 Constraint (Boundary) equations

Equation (2) for each link is subjected to constraint equations at both ends (u=0 or 1), which may be a floating and/or fixed joints shown in Fig. 2. For convenience, we introduce $\bar{u}$ and δ to denote the value of u at the joint so that

$$\delta = \begin{cases} -1 & \text{if } \bar{u} = 0 \\ +1 & \text{if } \bar{u} = 1 \end{cases}$$

For clarity, the constraint equations are divided into two classes, force/displacement and angle/moment, as follows:

1. Force/displacement constraint equations

Force/displacement constraints depend on the mobility of joints (floating or fixed). For a floating joint, the forces must balance regardless of its type (clamped or revolute). With external forces F_{xk} and F_{yk}, the followings must be satisfied:

$$\sum_{j=1}^{w} \delta h_j - F_{xk} = 0 \; ; \; \sum_{j=1}^{w} \delta v_j - F_{yk} = 0 \qquad (3a,b)$$

The links are also connected rigidly at the floating joint and must satisfy the following w-1 constraint equations.

$$\begin{aligned} x_j(\bar{u}_j) - x_{j+1}(\bar{u}_{j+1}) &= 0 \text{ for } j = 1 \sim w-1 \\ y_j(\bar{u}_j) - y_{j+1}(\bar{u}_{j+1}) &= 0 \text{ for } j = 1 \sim w-1 \end{aligned} \qquad (3c,d)$$

In addition, a floating joint may be subject to absolute displacement load (D_{xk}, D_{yk}) as follows:

$$x_1(\bar{u}_1) = D_{xk} \; ; \; y_1(\bar{u}_1) = D_{yk} \; . \qquad (3e,f)$$

When an arbitrary D_{xk} or D_{yk} is applied to a joint, the corresponding forces (F_{xk} and F_{yk}) are unknown since force and displacement cannot be applied simultaneously at a joint.

For a fixed joint, the two constraint equations are

$$x(\bar{u}) = \text{constant and } y(\bar{u}) = \text{constant} \; . \qquad (3g,h)$$

The internal forces for the link connecting to a fixed joint at one end must be determined from the other end, which connects to a floating joint.

2. Moment/Angle constraint equations

Moment/angle constraints given below depend on joints types (clamped or revolute as well as floating or fixed joints):

Floating joint - w constraint equations

At a *clamped joint*, the clamped angle between every two links must remain unchanged after they are deflected and the moment summation of every link must balance at the joint:

$$\begin{aligned} &\eta_j(\bar{u}_j) - \eta_{j+1}(\bar{u}_{j+1}) = [\psi_j(\bar{u}_j) + \gamma_j(\bar{u}_j)] - \\ &[\psi_{j+1}(\bar{u}_{j+1}) + \gamma_{j+1}(\bar{u}_{j+1})] \quad \text{where } j = 1, \cdots, w-1 \end{aligned} \qquad (4a)$$

$$\sum_{j=1}^{w} \delta \frac{EI_j}{L_j} \left[\psi_j'(\bar{u}_j) - \eta_j'(\bar{u}_j)\right] = 0 \qquad (4b)$$

A *revolute joint* cannot resist moment hence the change of slope must be zero for all the w links.

$$\left[\psi_j'(\bar{u}_j) - \eta_j'(\bar{u}_j)\right] = 0 \text{ for } j = 1 \sim w \qquad (4c)$$

Fixed joint - one constraint equation

Equation (4d) is the angle constraint for a clamped joint and (4e) is the moment equation for a revolute joint.

$$\eta(\bar{u}) = \psi(\bar{u}) \; ; \left[\psi'(\bar{u}) - \eta'(\bar{u})\right] = 0 \qquad (4d,e)$$

II.3 Forward and Inverse as a Dual Problem

The system (Figs. 1 and 2) represented by equations (2a-2h) and constraints (3) and (4) can be formulated as a forward or an inverse problem, which are a complementary pair as illustrated in Fig. 5.

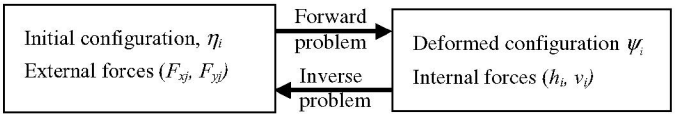

Fig. 5 Forward and inverse problems

The forward analysis solves for the deformed shape characterized by the link curvature $\psi_i + \gamma_i$ and the corresponding internal forces (h_i, v_i) given the initial shape η_i and external forces. On the other hand, the inverse analysis solves for the initial shape η_i and external forces given the deformed shape and internal forces. Unlike the forward model that focuses on analysis, the inverse model is for synthesis (or design). It is not always known how much an external force a mechanism can resist before it yields. However, the yield strength of common material is generally available. By specifying internal forces that are below the material's limit, the inverse analysis will give us the appropriate external forces. We present in the next section the generalized multiple shooting method for solving the forward/inverse models.

III. Generalized Multiple Shooting Method (GMSM)

Consider the following system of ℓ coupled, normalized sets of 1st order nonlinear ordinary differential equations:

$$\begin{bmatrix} \mathbf{M}_1 \mathbf{q}_1' \\ \vdots \\ \mathbf{M}_\ell \mathbf{q}_\ell' \end{bmatrix} = \begin{bmatrix} \mathbf{f}_1(u_1, \mathbf{q}_1, \xi_1) \\ \vdots \\ \mathbf{f}_\ell(u_\ell, \mathbf{q}_\ell, \xi_\ell) \end{bmatrix} \qquad (5)$$

where $0 \le u_i \le 1$ are independent variables; $i = 1, \ldots, \ell$;

$\mathbf{q}_i = [q_{i1} \quad q_{i2} \quad \cdots \quad q_{in}]^{\mathrm{T}}$ is the state vector, $\mathbf{q}_i' = d\mathbf{q}_i / du_i$;

$\mathbf{M}_i$ is the coefficient (mass) matrix; and

$\xi = [\xi_1^T, \xi_2^T, \cdots, \xi_\ell^T]^T$ is a vector of r unknown parameters.

If $\mathbf{M}_i$ is a singular matrix, then (5) is a differential-algebraic equation (DAE), otherwise it is an ODE. Each set of (5) governs the deformation of one link. We decompose (5) into N

sub problems by dividing the interval of integration [0 1] into N subintervals with N+1 nodes.

$$0 = u_{i1} < u_{i2} < \cdots < u_{ij} < \cdots < u_{iN} < u_{i,N+1} = 1\,;$$
$$i = 1,\ldots,\ell \ \text{ and } \ j = 1,\ldots,N+1$$

where u_{ij} denotes the normalized arc length of the j^{th} node in the i^{th} link. A single shooting method is performed in each subinterval of each link so that the resulting solution segments are connected to form a continuous solution over [0 1]. Figure 6 shows the idea of multiple shooting.

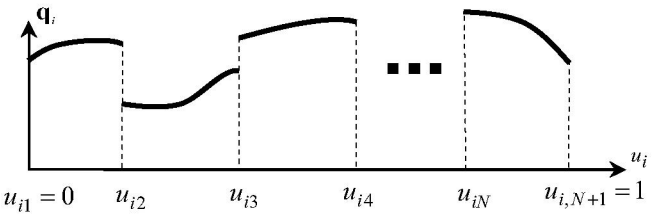

Fig. 6 Multiple shooting method

Since shooting is performed more than once in the overall interval, the method is called multiple shooting. It is also called parallel shooting because shooting method is performed independently on each subinterval.

Similar to single shooting, each subinterval of the multiple-shooting requires an initial set of values in order to integrate the ODE's. We denote the initial values of each subinterval as

$$\mathbf{q}(\mathbf{u}_j) = [\mathbf{q}_1^T(u_{1j}) \ \ \ldots \ \ \mathbf{q}_i^T(u_{ij}) \ \ \cdots \ \ \mathbf{q}_\ell^T(u_{\ell j})]^T$$
$$= \boldsymbol{\mu}_j = [\boldsymbol{\mu}_{1j}^T \ \ \ldots \ \ \boldsymbol{\mu}_{ij}^T \ \ \cdots \ \ \boldsymbol{\mu}_{\ell j}^T]^T \ \ ; \ 1 \le j \le N$$

where $\boldsymbol{\mu}_j$ now is an $\ell n \times 1$ vector. These initial values are not known in advance and treated as unknowns. For N subintervals we have $\ell n \times N$ unknown initial values

$$\boldsymbol{\mu} = [\boldsymbol{\mu}_1^T \ \ \ldots \ \ \boldsymbol{\mu}_j^T \ \ \cdots \ \ \boldsymbol{\mu}_j^T]^T$$

with r unknown parameters $\xi = [\xi_1^T, \xi_2^T, \cdots, \xi_\ell^T]^T$. The $\ell nN + r$ unknowns are related by the following equations:

(i) $\ell \times n$ boundary constraint equations correspond to (3c~3g) and (4a~4e):

$$\mathbf{g}(\mathbf{q}(0), \mathbf{q}(1)) = 0 \tag{6a}$$

(ii) $(N-1)n\ell$ continuity equations connect the solution segments together:

$$\boldsymbol{\mu}_{j+1} = \mathbf{q}(\mathbf{u}_{j+1}; \boldsymbol{\mu}_j) \ \ j = 1 \sim N+1 \tag{6b}$$

We put $\boldsymbol{\mu}_j$ after the semicolon to express that the value $\mathbf{q}(\mathbf{u}_{j+1})$ is a function of the initial value $\boldsymbol{\mu}_j$ in the j^{th} interval.

(iii) r geometric constraint equations for r unknown parameters correspond to (3a, 3b).

$$\mathbf{g}(\boldsymbol{\mu}, \xi) = 0 \tag{6c}$$

Combining (6a), (6b), and (6c) leads to a set of $\ell nN + r$ nonlinear algebraic equations as follows:

$$\mathbf{F}(\boldsymbol{\mu}, \xi) = \begin{bmatrix} \boldsymbol{\mu}_2 - \mathbf{q}(\mathbf{u}_2; \boldsymbol{\mu}_1) \\ \boldsymbol{\mu}_3 - \mathbf{q}(\mathbf{u}_3; \boldsymbol{\mu}_2) \\ \vdots \\ \boldsymbol{\mu}_N - \mathbf{q}(\mathbf{u}_N; \boldsymbol{\mu}_{N-1}) \\ \mathbf{g}(\mathbf{q}(\mathbf{u}_1; \boldsymbol{\mu}_1), \mathbf{q}(\mathbf{u}_{N+1}; \boldsymbol{\mu}_N)) \\ \mathbf{g}(\boldsymbol{\mu}, \xi) \end{bmatrix} = 0 \tag{7}$$

In summary, the GMSM includes four steps:

(i) Recast the BVP in a state-space form as (5).
(ii) Identify unknown initial values and parameters.
(iii) Formulate constraint equations from (3) and (4).
(iv) Integrate (5) and solve for unknowns in (7).

The GMSM can be solved iteratively by methods such as Newton's or Quasi-Newton, where (5) is integrated in each iteration. Using the steps given above, we solve (2) using GMSM as will be illustrated in the following section.

IV. Forward And Inverse Analyses

We consider the forward and inverse problems separately since they have different state-space forms.

IV.1 Forward and inverse models in state-space forms

The forward problem is defined as follows: *Given initial mechanism configuration and external loads, solve for the deformed configuration and internal forces of all links*. For this, equations (2a)~(2f) are recast in a state-space form:

$$\mathbf{M}_i \mathbf{q}_i' = \begin{bmatrix} \psi' \\ {}^{L_i^2}\!/_{EI_i}[h_i \sin(\psi_i + \gamma_i) - v_i \cos(\psi_i + \gamma_i)] + \eta'' \\ L_i \cos(\psi_i + \gamma_i) \\ L_i \sin(\psi_i + \gamma_i) \\ [v_i \cos(\psi_i + \gamma_i) - h_i \sin(\psi_i + \gamma_i)] - \kappa_i G A_i \gamma_i \end{bmatrix} \tag{8a}$$

where $\mathbf{q}_i = [\psi \ \ \psi' \ \ x \ \ y \ \ \gamma]^T$ are the state variables. Since the last component in (8a) is an algebraic equation that does not include γ', the matrix $\mathbf{M}_i$ is singular. Equation (8a) becomes a set of DAE. MATLAB program ode15s and ode23t [10] can be used to integrate DAE as an ODE.

We define the inverse problem as follows: *Given a deformed configuration and some of its internal forces, solve for the initial configuration and external forces.* The internal forces are the design parameters to be specified (with selection of materials). As in the forward analysis, equations (2a)~(2d) and (2g,h) are recast for the inverse problem in (8b):

$$\mathbf{M}_i \mathbf{q}_i' = \begin{bmatrix} \eta' \\ {}^{L_i^2}\!/_{EI_i}[v_i \cos(\psi_i + \gamma_i) - h_i \sin(\psi_i + \gamma_i)] + \psi'' \\ L_i \cos\eta_i \\ L_i \sin\eta_i \\ [v_i \cos(\psi_i + \gamma_i) - h_i \sin(\psi_i + \gamma_i)] - \kappa_i G A_i \gamma_i \end{bmatrix} \tag{8b}$$

where $\mathbf{q}_i = [\eta \ \ \eta' \ \ x \ \ y \ \ \gamma]^T$ are the state variables. Opposite of (8a), the unknown and known shape functions of the inverse problem are η and ψ respectively.

IV.2 Number of unknowns and constraint equations

The unknowns generally include initial values of (8) with force loads (F_{xk}, F_{yk}) and/or displacement loads (D_{xk}, D_{yk}). As an example, we consider force loads for the mechanism shown in

Fig. 1. The number of constraint equations and unknowns are given in Tables 1 and 2.

Table 1 Number of constraint equations for a joint

Type of joints	Floating joint	Fixed joint
Force/displacement	$2w$	2
Moment/angle	w	1
Total	$3w$	3

Table 2 Unknowns for the forward and inverse problem

Type of unknowns	Forward problem	Inverse problem
Initial values (μ)	$\psi_i(0)$, $\psi_i'(0)$, $x_i(0)$, $y_i(0)$	$\eta_i(0)$, $\eta_i'(0)$, $x_i(0)$, $y_i(0)$
Parameters (ξ)	h_i , v_i	h_i , v_i , F_{xk} , F_{yk}
# of unknowns	6ℓ	6ℓ

The number of constraint equations is independent of problem types, i.e., a floating joint connecting w links will have $3w$ constraint equations while a fixed joint will have three. For a forward problem where external forces are given, there are 6 unknown for every link and hence a mechanism with ℓ links will have 6ℓ unknowns. In order to apply GMSM, we provide the proof that the number of unknowns is always equal to that of the constraint equations for a forward problem.

Proof: Consider a mechanism consisting of ℓ links. Then the total number of connections is equal to 2ℓ as a link has two connections. For n_i floating joints connecting i links and m fixed joints, the sum of these joints must equal to the number of connections, or

$$2\ell = \sum_{i=2}^{\ell} in_i + m \text{ ; and } 6\ell = \sum_{i=2}^{\ell} 3in_i + 3m \qquad (9, 10)$$

Equation (10) is the result of multiplying (9) by three on both sides, where the 1st and 2nd terms on the right hand side represent the number of constraint equations from floating joints and fixed joints respectively. The sum of them equals to 6ℓ (number of unknowns) on left hand side. We then finish the proof. The forward problem is always solvable.

For the inverse problem where some of the internal forces are given, the number of unknowns must also equal to 6ℓ. In order to be solvable, the number of given internal forces must be equal to the number of unknown external forces. For the case of one external force, we specify the internal force of the link that undergoes most critical loads. Note that the internal force and the applied force don't have to act on the same joint. For cases of multiple external forces, care must be taken so that the specified internal forces are not over-constrained.

V. Illustrative Examples and Applications

We demonstrate GCM and its forward/inverse models with three examples. The 1st example illustrates the effect of shear deformation on the link deflection. The 2nd and 3rd examples illustrate the forward and inverse analyses respectively.

Example 1: Effect of shear deformation on link deflection

As shown in (2d~f), the link deflection is caused by both bending and shear. Although shear angles are small within each infinitesimal element, they accumulate along the axial direction of the link. The effect of shear deformation at the tip can be observed by comparing the computation with/without shear deformation, which cannot be ignored especially for highly compliant members or precision flexure mechanisms.

We investigate the effect of shear deformation by applying a vertical ($+y$) force on a compliant link originally pointing to $+x$. We denote $\delta+\delta_s$ and δ as the tip deflections in the $+y$ with and without considering shear deformations. We use κ=5/6 as the shear correction factor for rectangular cross-sections. Other shear correction factor can be found in [11].

It can be shown from (2d) that the shear angle is inverse proportional to shear modulus G, and from (2a, d) that the shear angle is proportional to the square of the link height h. We define the following two ratios so that the effect of these two factors on the shear deformation can be studied on a non-dimensional basis:

(a) Material property ratio (E/G): This ratio is related to Poisson's ratio as $E/G=2(1+v)$. Typical materials have an E/G between two to three, such as steel (E/G=2.54), Delrin (E/G=2.7), and rubber (E/G=3).

(b) Geometric aspect ratio (h/L).

Figure 7 shows the effects of these two ratios on the tip deflection for δ=0.2. Figure 8 shows the effect of increasing tip deflection δ to the deflection δ_s caused by shear.

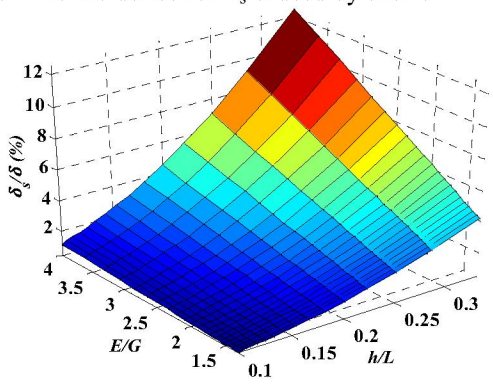

Fig. 7 Effect of shear on tip deflection with δ=0.2

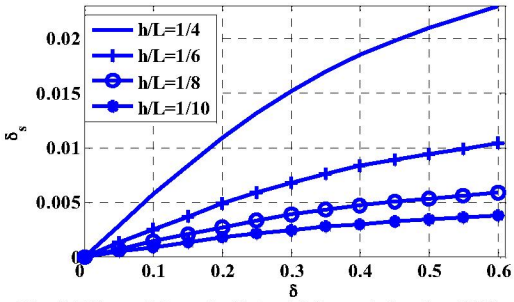

Fig. 8 Effect of shear for link with large deflection (E/G = 3)

Clearly, the deflection δ_s becomes more significant as the two ratios increase; it is especially dominated by the geometric ratio. As expected, δ_s increases as δ increases. Hence the tip deflection due to shear deformation becomes significant for links undergoing large deflections.

Example 2: Forward analysis of a compliant grasper

An application of the GCM is to analyze a compliant grasper (shown in Fig. 9) for handling objects. The pair of compliant links shown in Fig. 9(a) have an initial shape $\eta(u)=1.33\sin(2\pi u)$. They support the rigid frame that has compliant fingers mounted (not shown in Fig. 9(b~c)). By the contact forces from the object to the fingers, the links deform to accommodate objects with variable sizes and shapes.

Due to symmetry, we analyze the right hand side of the grasper. The sinusoidal link clamped at J_1 and J_2 has length L=0.085m and Young's modulus E=2.62GPa (Delrin). The link also has thickness 0.001016m and width 0.04572m.

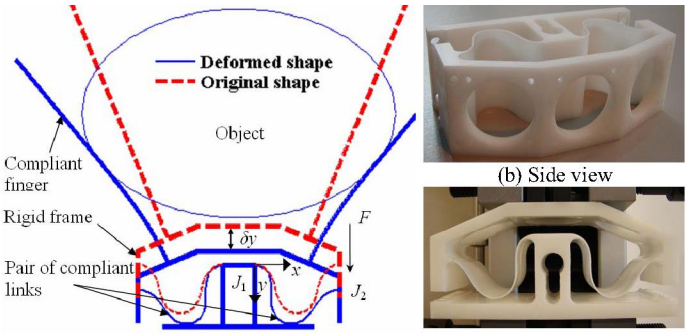

(a) Gripping with a compliant grasper

(b) Side view

(c) Deformed shape

Fig. 9 A compliant grasper

We solve for the displacement δy of the rigid frame given force F at J_2. Since the mechanism consists of $\ell = 1$ link, there are 6x1=6 constraint equations. The computed F-δy curve is shown in Fig. 10. The results match well with those obtained by an experiment, where both tension and compression tests are performed.

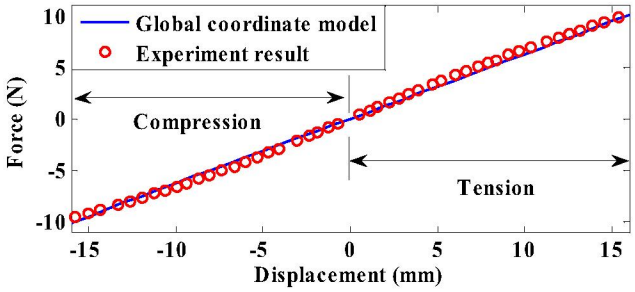

Fig. 10 Validation of force-displacement relations

Example 3: Inverse analysis of a four-bar mechanism

Consider a compliant 4-bar mechanism. The interest is to find a configuration that, after deflected, has the shape shown in Fig. 11. It is required that L_2 remains straight under an external force F_{x2}. We also know the maximum stress of the material before yield is $\bar{\sigma}$. Since the maximum stress occurs at the ends of links, we express the stress at, say, J_1, as

$$\sigma_{\max} = \frac{Mc}{I} = \frac{c\{v_1 x_1(1) - h_1 y_1(1) + EI_1 / L_1[\psi_1'(1) - \eta_1'(1)]\}}{I_1} < \bar{\sigma}$$

We use 0.1 as the safety factor and hence $\sigma_{\max} = 0.1\bar{\sigma}$. We now seek for the original shape and F_{x2} that will give us the required maximum stress. The parameters of the 4-bar mechanism are $EI_1 = EI_2 = EI_3 = 0.08\text{Nm}^2$, $L_1 = L_3 = 0.2$m, $L_2 = 0.1932$m, c=2mm, $\bar{\sigma}$ =48.4MPa.

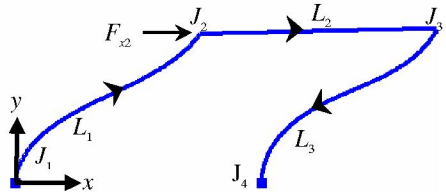

Fig. 11 Deformed shape of a four-bar mechanism

As the deformed shape is known, the angles of each link can be approximated as a 4th order polynomial shown in Table 3.

Table 3 Polynomials that approximate the angle functions

L_1	$\psi_1(u_1) \approx 4.88u_1^4 - 11.09u_1^3 + 11.36u_1^2 - 5.74u_1 + 1.56$
L_2	$\psi_2(u_2) = 0.0233$
L_3	$\psi_3(u_3) \approx -0.43u_3^4 + 0.73u_3^3 + 3.30u_3^2 - 3.10u_3 - 2.06$

By using the approach stated in Section II.2, we formulate the 3x6=18 constraint equations. The external force F_{x2} is now an unknown and we specify the value of h_3. The total number of unknowns is 18, which matches the number of constraint equations. Two original shapes are obtained in Fig. 12 for h_3=5N and h_3= -5N. Their required forces are 32.48N and -32.33N respectively.

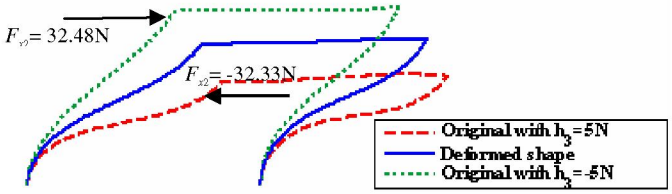

Fig. 12 Original and deformed shape of the four-bar mechanism

VI. Conclusions

We present the global coordinate model (GCM) along with an improved numerical solver (GMSM) to analyze and design the configuration of a compliant link under external loads. The GCM, which takes into account both flexural and shear deformation, can be viewed as a generalization of Timoshenko's beam equations. The effect of shear deformation on the deflection of a compliant link has been characterized. When applying to multiple links, the GCM requires only one coordinate and thus simplify the formulation. The GCM, which is capable of both forward and inverse analysis, consists of a systematic formulation for analytical design of generic compliant mechanisms. It is expected that the systematic approach presented here has a broad application in designing compliant mechanisms.

References

[1] Howell, L. L., 2001, *Compliant Mechanisms*, John Wiley & Sons.

[2] Rankin, C. C. and Brogan, F. A., 1986, "An Element Independent Corotational Procedure for the Treatment of Large Rotations," ASME J. Pressure Vessel Technology, **108**, pp. 165-174.

[3] Shabana, A. A., 1998, Dynamics of multibody systems, Wiley, N.Y.

[4] Stack, K. D., Benson, R. C., and Diehl, T., 1994, "*The Inverse Elastica Problem and its Application to Media Handling*," ASME International Mechanical Engineering Congress and Exposition, **186**, pp. 31-36.

[5] Saggere, L. and Kota, S., 2001, "Synthesis of Planar, Compliant Four-Bar Mechanisms for Compliant-Segment Motion Generation," ASME Journal of Mechanical Design, **123**, pp. 535-541.

[6] Lan, C.-C., Lee, K.-M., 2005, "*Generalized Shooting Method for Analyzing Compliant Mechanisms*," IEEE International Conference on Robotics and Automation, Barcelona, Spain.

[7] Keller, H. B., 1968, Numerical Methods for Two-Point Boundary-Value Problems, Blaisdell publishing, Waltham, MA.

[8] Yin, X., Lee, K.-M., and Lan, C.-C., 2004, "Computational Models for Predicting the Deflected Shape of a Non-Uniform, Flexible Finger," *IEEE ICRA*, New Orleans, **3**, pp. 2963-2968.

[9] Frisch-Fay, R., 1962, *Flexible Bars*, Washington, Butterworths.

[10] Shampine, L. F., Reichelt, M. W., and Kierzenka, J. A., 1997, "*Solving Index-1 DAEs in MATLAB and Simulink*," SIAM Review, **41**(3), pp. 538.

[11] Kaneko, T., 1975, "*On Timoshenko's Correction for Shear in Vibrating Beams*," J. Phys. D: Appl. Phys., **8**, pp. 1927-1936.

[12] Kim, C., Kota, S., 2002, "*Design of a Novel Compliant Transmission for Secondary Microactuators in Disk Drives*," ASME International Design Engineering Technical Conferences, Montreal, CA.